Journal of Thermal Analysis and Calorimetry, Vol. 88 (2007) 1, 261–267

THERMAL AND MECHANICAL-INDUCED PHASE TRANSFORMATIONS DURING YAG AND ALUMINA–YAG SYNTHESES

Paola Palmero[*] *and Laura Montanaro*

Politecnico of Torino, Department of Materials Science and Chemical Engineering, INSTM – R.U. PoliTO – LINCE Lab.
Corso Duca degli Abruzzi, 24-10129 Torino, Italy

The preparation of pure $Y_3Al_5O_{12}$ (YAG) and 50 vol% Al_2O_3–YAG composite powders by a wet chemical route is presented. The role of the synthesis temperature during reverse-strike precipitation has been investigated, showing its relevant effect on the purity and homogeneity of YAG powder.

The composite material was prepared by comparing two different synthesis routes. A composite powder was synthesized via reverse-strike temperature-controlled co-precipitation. In the latter case, a pure-alumina precursor was firstly reverse-strike precipitated and then doped with an yttrium salt solution. For both syntheses, the role of thermal and mechanical pre-treatments on the phase development was demonstrated.

Keywords: *alumina–YAG composites, powder processing, synthesis routes, thermal evolution*

Introduction

Yttrium aluminum garnet ($Y_3Al_5O_{12}$, YAG) as well as alumina–YAG composites are strongly promising for optical, electronic and low or high-temperature structural applications [1, 2] as evidenced by the variety of investigations during the last decade on pure-phased YAG [3–7] and on alumina–YAG composite powder preparation [8, 9].

Traditional solid-state reaction from oxide mixture requires high-temperature processing to obtain pure YAG [10], leading to uncontrolled microstructural features. On the contrary, an increase in purity and a lowering in the crystallization temperature have been recently pursued by using wet chemical methods: among them, the reverse-strike co-precipitation has been shown as one of the most successful [11–14]. In spite of this, various processing parameters should be optimised and strictly controlled during this synthesis to assure homogeneity and reproducibility of the final products [11, 14].

In this paper, a pure-YAG powder was synthesized by reverse-strike co-precipitation, through the optimisation of some synthesis parameters, such as precipitation pH, solution concentration and rate of the solution addition into the precipitant medium. In addition, the role of the synthesis temperature on the crystallization path was investigated in a systematic way, for a sake a comparison with literature data on pure-alumina synthesis which underline the strong influence of temperature on phase evolution during calcination [15–17]. In fact such data are still partially lacking for what concerns YAG phase. The set-up of the synthesis procedure of alumina–YAG composite powders was then achieved by exploiting the above knowledge.

The second part of this paper therefore deals with the preparation of 50 vol% alumina–YAG composite powders by following two different synthesis routes.

In the first case a composite precursor was reverse-strike co-precipitated following the procedure set up for pure YAG. For a sake of comparison, the second composite powder was prepared starting from a pure-alumina precursor precipitated by using a reverse-strike procedure and then doped with a stoichiometric amount of yttrium nitrate.

For both syntheses, the role of thermal and mechanical pre-treatments on the phases development has been investigated.

Experimental

Materials and methods

Reverse-strike co-precipitation

A pure-YAG precursor was prepared by reverse-strike co-precipitation, starting from an aqueous chloride solution containing Y and Al ions in a molar ratio of 3:5. For the simultaneous and quantitative precipitation of both aluminium and yttrium hydroxides, the starting solution was added dropwise to an aqueous ammonia solution kept at a constant pH value of 9. Fluctuations around the

* Author for correspondence: paola.palmero@polito.it

1388–6150/$20.00

Akadémiai Kiadó, Budapest, Hungary
Springer, Dordrecht, The Netherlands

fixed pH value were controlled in a range ±0.2 by a pH-meter (Orion, model SA520), by adding extra-ammonia solution (4M). After precipitation, the gelatinous product was washed four times with dilute ammonia at pH 9 and twice with absolute ethanol before drying in oven at 60°C for 48 h. Three different syntheses were performed at 5°C, 25°C and 60°C with the aim of studying the influence of the precipitation temperature on the phase evolution in samples labelled respectively YAG5, YAG25 and YAG60. More details on this synthesis were already given elsewhere [18]. The dried powders were characterised by DTA/TG simultaneous analysis (Netzsch STA 409C, heating and cooling rate of 10°C min^{-1} in static air up to 1400°C) and calcined at various temperatures for different times: the phase evolution was studied by X-ray diffraction (XRD, Philips PW 1710) and the crystallite growth was followed by TEM (Jeol 200 CX) observations.

On the ground of these results, the best synthesis temperature (25°C) was selected, and the set-up procedure was then applied for the preparation of 50 vol% alumina–YAG composite powders (labelled powder R), starting from an aqueous chloride solution which contained Y and Al ions in a molar ratio of 3:15. The crystallization path was evidenced by means of XRD analysis performed on the differently calcined powders and compared to that of a system having the same composition but prepared with a different procedure: the post-doping method, as reported in the following.

Post-doping route

A pure-alumina precursor was synthesized by using the same reverse-strike temperature-controlled procedure, that is adding an aqueous solution of $AlCl_3 \cdot 6H_2O$ to an ammonia solution kept at a constant pH of 9. This powder, labelled A, was fully characterized as previously described for powder R. The dried precipitate was then planetary milled in absolute ethanol with agate balls and vessels for 12 h (powder A1). The mean particle size distribution was evaluated by laser granulometry (Fritzsch analysette 22 compact), after ultrasonic dispersion in absolute ethanol for 10 min. Alumina–YAG composite powders were then prepared by adding a stoichiometric amount of yttrium nitrate ($Y(NO_3)_3 \cdot 6H_2O$), to absolute ethanol suspensions of the un-calcined A1 powder as well as of powder A1 treated at different temperatures on the ground of XRD data and related phase evolution. The doped powders, labelled powders D, yielded the final phases, α-Al_2O_3 and YAG, by subsequent firing as a result of nitrate decomposition and solid-state reactions. The reaction path of the doped precursor pre-treated in different conditions (just dried or even calcined up to induce partial crystallization of transition and/or α-alumina) were compared and strongly different crystallization paths were observed. Surface activation by an extensive milling of pure and doped-powders treated at different temperatures also induced different crystallization paths through the final phases.

Results and discussion

Pure-YAG powders

XRD analysis on the as-dried products revealed that YAG5 and YAG25 were completely amorphous, whereas traces of bayerite were detected in YAG60. These results are in partial agreement with the studies performed on pure alumina precursor in which the formation of highly crystalline precipitate is favored by the higher synthesis (precipitation or hydrolysis) temperatures [15, 17].

Simultaneous DTA-TG characterization was performed on the three synthesized materials: in spite of both thermal data have been considered for the following discussion, in Fig. 1 only the DTA curves in the high-temperature range of the three materials after thermal pre-treatment at 800°C for 0 h have been reported, with the aim to evidence better the exotherms associated to the crystalline phases appearance. However, more detailed information on the thermal behaviour of such synthesized powders have been reported in a previous paper [18].

For the three powders, a strong exotherm followed by a broad and slightly intense signal at higher temperature could be observed. As previously proposed by Yagamuchi *et al*. [19], the sharp peak at about 900°C can be associated to the crystallization of the metastable hexagonal $YAlO_3$ phase (h-$YAlO_3$), whereas the broader and less intense peak at higher temperature can be attributed to the transition from the hexagonal phase to the 3:5 garnet-structured YAG. Such phase evolution has been confirmed by XRD analyses performed on the three powders calcined in that temperature range (Fig. 2), as described

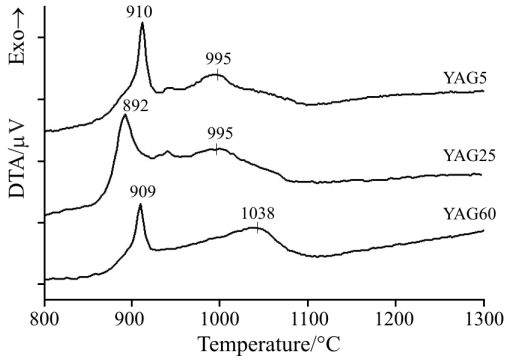

Fig. 1 DTA curves of the 800°C pre-treated YAG5, YAG25 and YAG60 powders

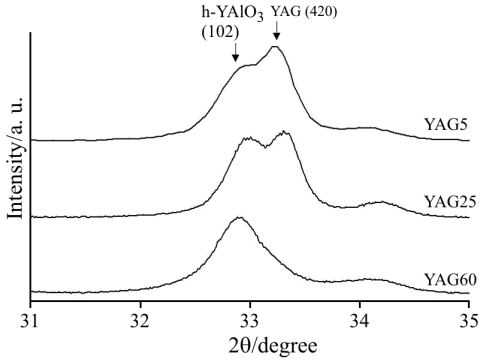

Fig. 2 XRD patterns of as-synthesized YAG5, YAG25 and YAG60 calcined at 915°C for 0 h

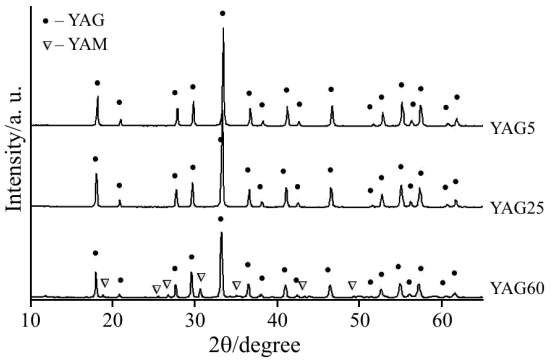

Fig. 3 XRD patterns of YAG5, YAG25 and YAG60 calcined at 1350°C for 0.5 h

below. Although similar exothermal signals could be observed for the three materials, some differences in the crystallization temperatures of the yttrium aluminates could be remarked. The main differences could be observed in the slightly lower h-$YAlO_3$ crystallization temperature for YAG25 and in the significantly higher transformation temperature of the metastable phase into the YAG phase in YAG60 material. In addition, a small intermediate peak at about 950°C appears in the curve of YAG5 and YAG25, but XRD analysis on samples calcined at this temperature did not allow to relate it to a new phase appearance.

The different phase evolution as a function of the synthesis temperature has been evidenced more systematically by means of XRD investigation on powders calcined in their crystallization temperature range. Figure 2 reports the XRD patterns in the 31–35° 2θ range, where the more intense h-$YAlO_3$ and YAG peaks appear, for the three materials pre-treated at 915°C for 0 h.

In sample YAG5, the simultaneous appearance of the peaks attributed to h-$YAlO_3$ and YAG was identified; however, at this temperature, YAG peaks are higher than those of hexagonal phase. Also in the case of YAG25, the same phases are yielded at 915°C but, in this case, the intensities of h-$YAlO_3$ and YAG peaks are quite the same. On the contrary, YAG60 crystallises at 915°C yielding only the h-$YAlO_3$. After higher-temperature treatments (namely at 1100°C for 0 h or 1350°C for 0.5 h) pure YAG is the only phase detected in YAG5 and YAG25, whereas it is the prevalent one near monoclinic $Y_4Al_2O_9$ (YAM) phase in YAG60. To have a better evidence of the secondary phase in YAG60, Fig. 3 reports the full-range XRD pattern on the three powders calcined at 1350°C for 0.5 h.

Other interesting features were observed by performing thermal treatments at the same temperature (850°C) but for different soaking times (0.5, 1 and 4 h), as reported in Figs 4a–c. In the case of YAG5, after 30 min soaking at 850°C, the garnet is well crystallized near less pronounced h-$YAlO_3$ peaks. The intensity of the YAG peak increases with increasing the soaking time, accompanied by a decreasing intensity of the hexagonal phase. This material yielded an almost pure product after 4 h-soaking step, whereas only traces of the metastable phase could be detected. In YAG25 both phases crystallise during 0.5 h soaking; however, when the sample is treated for longer times at this temperature, the amount of YAG monotonically increases, whereas the h-$YAlO_3$ phase does not change significantly. In the sample YAG60, h-$YAlO_3$ is the only crystallised phase after 30 min soaking. This is the prevalent crystalline phase present in the sample even after 4 h, while the YAG phase is still in traces. More detailed information on the phase evolution of such synthesized powders have been reported in a previous paper [18], in which XRD results were also confirmed by TEM observations and electron diffractions performed on powders calcined at different temperatures.

These results showed that pure-YAG phase could be obtained by controlling the synthesis temperature in the range 5–25°C. The precipitation performed at 60°C leads to an increase in crystallization temperature for the YAG phase; in addition YAG60 appears to be less pure than the other products: after high-temperature calcination it yields a biphasic final product and the traces of bayerite phase in the dried product are probably a signal of a lower starting homogeneity.

50 vol% Al_2O_3–YAG by reverse-strike co-precipitated powders: powder R

On the ground of the previous results, a precursor of the composite material was produced by reverse-strike co-precipitation, at the constant temperature of 25°C.

In the as-dried product traces of the bohemite phase were detected by XRD and also confirmed by electron diffraction patterns by TEM analysis. DTA curve (Fig. 5) revealed in the high temperature range the presence of three exotherms at about 970, 1100 and 1250°C. In order to associate DTA signals to the

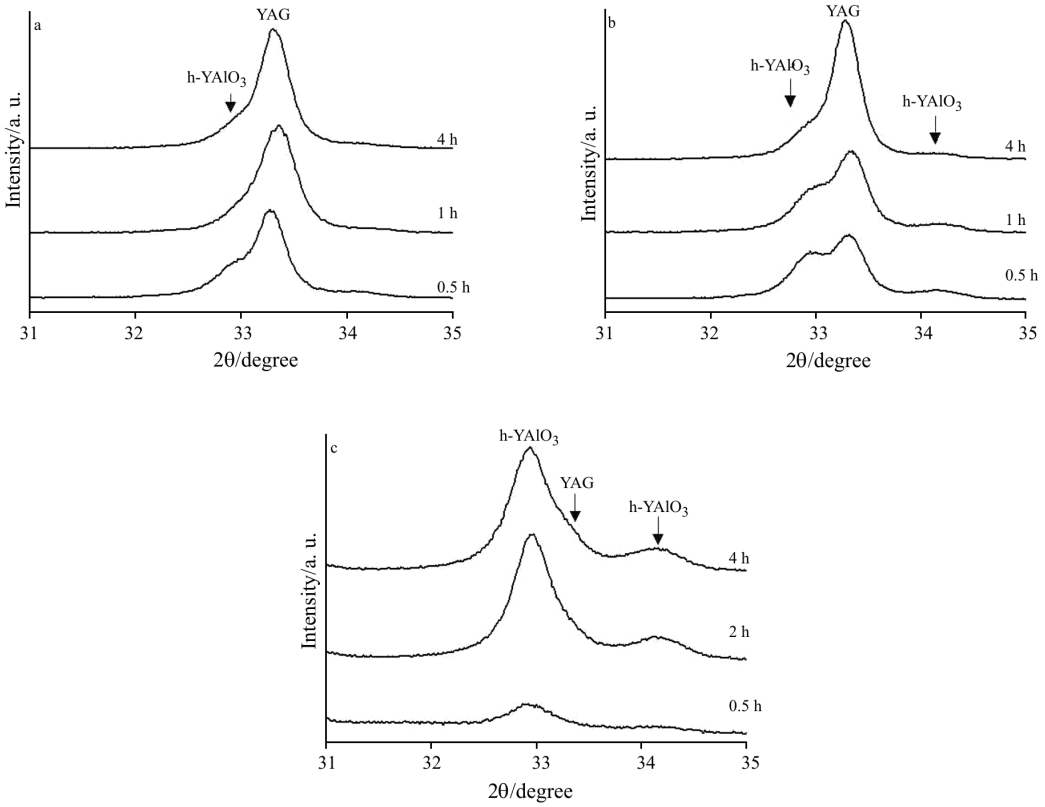

Fig. 4 XRD patterns of the a – YAG5, b – YAG25 and c – YAG60 calcined at 850°C for 0.5, 1 and 4 h

phases crystallization, XRD analysis were performed on the powder pre-treated at 980, 1120, 1215°C for 0 h and 1300°C for 0.5 h (Fig. 6).

In powder R, firstly the hexagonal h-$YAlO_3$ phase crystallises, in form of traces, at about 980°C. Traces of the YAG phase appear after calcination at 1120°C and its amount increases with the temperature. The XRD patterns of the powder calcined at 1215°C contained reflections of YAG and α-Al_2O_3 traces. Finally, in the powder calcined at 1300°C, well crystallised YAG and α-Al_2O_3 phases were detected. From these results it appears that the co-precipitation route allows the production of highly-pure alumina–YAG composites, since no other secondary stable or metastable phases were detected, even after high-temperature treatments. More detailed information about this synthesis could be found in a previous paper [20], in which TEM analysis allowed to observe the appearance of nanosized grains and to follow their growth as a function of calcinations temperatures.

50 vol% Al_2O_3–YAG by post-doping route: powder D

After drying, in the as-precipitated alumina precursor (powder A) bayerite and gibbsite were detected by XRD analysis. This result is a good agreement with literature

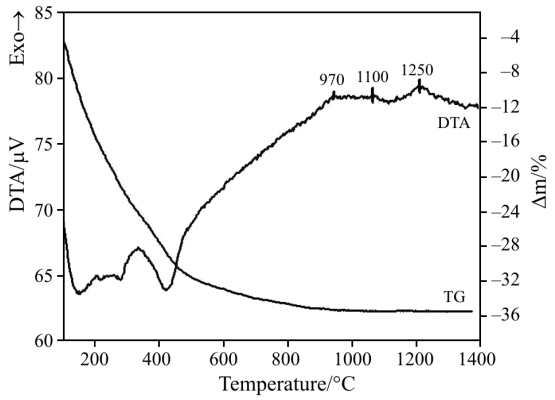

Fig. 5 DTA-TG curve of the as-dried powder R

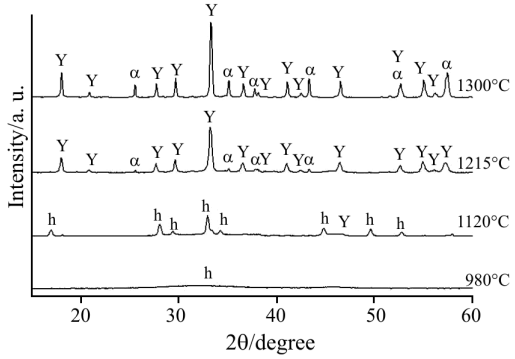

Fig. 6 XRD patterns of powder R calcined at 980, 1120, 1215°C for 0 h and 1300°C for 0.5 h; (Y=YAG, h=hexagonal $YAlO_3$, α=α-Al_2O_3)

data in which well-crystallized alumina precursor has been obtained at the higher precipitation pH [15, 21].

DTA analysis performed on the as-dried product (powder A) showed an exothermal signal at about 1285°C, which has been associated to α-Al_2O_3 crystallization, as confirmed by XRD analysis. However, if the same precursor was submitted to a planetary milling step for 12 h (in absolute ethanol and by employing agate vessels and balls; powder A1), a clear decreasing of α-Al_2O_3 crystallization temperature was observed, since the DTA exotherm was displaced to about 1165°C. This phenomenon was not observed in powder R: in fact, extensive milling steps on the just-dried or even calcined product did not induce any shift of crystallization temperature.

Powder A1 was then calcined at three different temperatures and times, in order to obtain only transition alumina (γ-Al_2O, by calcination at 500°C for a zero soaking time; powder A1-500), an incipient crystallization of α-Al_2O_3 (by calcination at 900°C for 30 min, powder A1-900) and a well crystallized α-Al_2O_3 (by calcination at 1280°C for 5 min, powder A1-1280), as stated by XRD (Fig. 7).

Alumina–YAG composite powders were then prepared by adding the stoichiometric amount of yttrium nitrate – dissolved in absolute ethanol – to the above powders, yielding the corresponding composite materials D1, D1-500, D1-900 and D1-1280. These doped powders were then treated in the temperature range between 1000 and 1300°C (for a zero soaking time) and XRD was performed to follow the phase evolution. A clear influence of the thermal pre-treatment of powder A1 on the crystallization path was stated, as shown in Table 1.

YAG crystallization temperature increases with increasing the pre-treatment temperature of powder A1. In addition, when powder A1 is calcined at the higher temperatures and then doped (i.e., D1-900 and D1-1280), the appearance of secondary, stable as well as metastable phases (like $Y_4Al_2O_9$, YAM; orthorhombic $YAlO_3$, YAP; Y_2O_3) was observed. On the contrary, calcination of powders D1 and D1-500 led firstly to the crystallization of the hexagonal phase, h-$YAlO_3$, that transforms into YAG phase at relatively low temperature, and then to pure α-alumina and YAG composite powders, similarly to powder R. The pure, final phases were yielded between

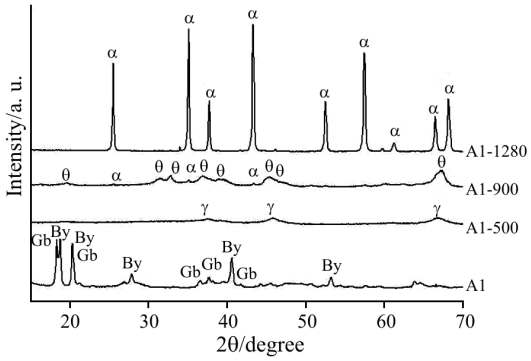

Fig. 7 XRD patterns of A1, A1-500, A1-900 and A1-1280 powders (Gb=gibbsite, By=bayerite, γ=γ-Al_2O_3, θ=θ-Al_2O_3, α=α-Al_2O_3)

1100 and 1200°C in doped-D1 powder and between 1200 and 1300°C in doped D1-500 powder.

In addition, some other interesting features could be observed by coupling mechanical and thermal pre-treatments on the doped powders, as reported in the following for the best performing materials which were D1 and D1-500 powders.

In fact, the above materials were planetary milled for 8 h (in absolute ethanol and using agate milling media) prior to be calcined in the 1000–1200°C temperature range. Figure 8 compares the XRD patterns of the un-milled D1 and powder D1 planetary milled for 8-h, after calcination at 1000, 1100 and 1200°C (zero soaking time).

Extensive milling led to a higher powder reactivity, since at all the investigated temperatures the yttrium aluminates phases were better crystallized in the milled powder. After calcinations at 1000°C, in milled D1 powder h-$YAlO_3$ phase was yielded, whereas it was not detected in the un-milled material. After calcination at 1100°C, an almost pure and quite well crystallized garnet structure was identified in the milled powder, whereas a still significant amount of the hexagonal phase was also present in the un-milled one. Finally, after calcinations at 1200°C, almost the same phase composition was obtained in both materials. α-Al_2O_3 crystallization, on the contrary, was not affected in a significant way by the milling step. A similar crystallization path was identified in milled D1-500 material, in which both h-$YAlO_3$ and YAG phase were better crystallized after calcination at 1000 and 1100°C as regards to the un-milled powder.

Table 1 XRD data of doped-D1 powders calcined at different temperatures

Calcination temp./°C	D1	D1-500	D1-900	D1-1280
1000	δ+h(t)+α(t)	δ	YAM+α(t)+θ	α+Y_2O_3+YAM(t)
1100	YAG+h+α+θ	h+YAG(t)+α(t)+δ	h+YAM+YAP+α(t)	α+YAM+YAG(t)+YAP(t)
1200	YAG+α+θ(t)	YAG+α(t)+θ	YAG+h+YAP+α	YAG+α+YAP+YAM
1300	YAG+α	YAG+α+θ(t)	YAG+α+YAP(t)	YAG+α

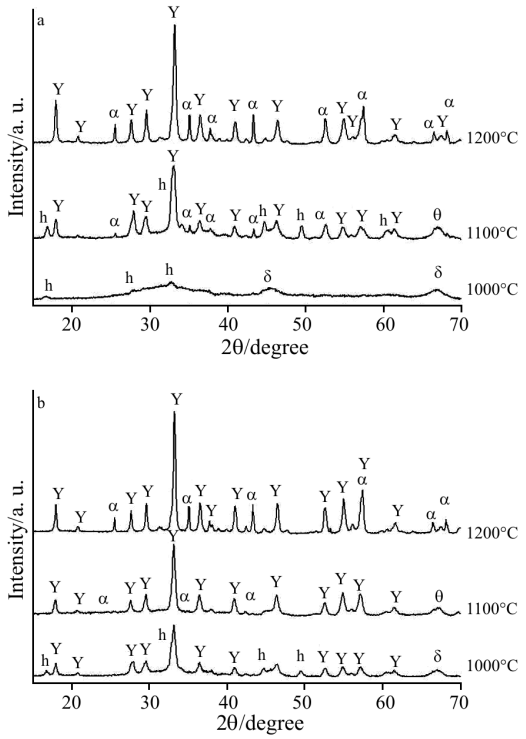

Fig. 8 XRD patterns of the a – un-milled D1 and b – 8 h planetary milled D1 powders after calcinations at 1000, 1100 and 1200°C for 0 h

The above results could not be attributed to a significant reduced agglomerate size after milling since both powders showed almost super-imposable particle size distributions with agglomerate sizes of about 0.8, 4 and 11 μm corresponding to 10, 50 and 90%, respectively, of the cumulative distribution.

The above results support this synthesis route as a valid alternative to the co-precipitation method; in addition, it could be exploited for a mass production of composite powders by using commercial transition alumina powders, as starting powder A. However, it needs the set-up of suitable thermal and mechanical pre-treatments in order to promote crystallization of YAG and α-Al_2O_3 at low temperature as well as to avoid the appearance of undesired secondary phases.

Finally, it should be pointed out that, for a sake of comparison, in this work pure alumina powder was synthesized at a pH of 9, as for pure-YAG and alumina–YAG materials; this condition led to a partially crystallized precipitate, as already stated in literature [15, 21]. An advancement in final product homogeneity could be reasonably achieved by doping a completely amorphous alumina precursor, precipitated in modified conditions [21].

Conclusions

From the above results the following conclusions can be drawn out:

- Reverse-strike co-precipitation of YAG powder was performed at three different temperatures (5, 25, 60°C) leading to products which mainly differ in terms of crystallisation temperature, phase evolution as a function of the heat treatment and soaking time, and final homogeneity. All the powders yielded YAG after calcination at 1100°C; however, in the case of YAG60, the product was less pure since $Y_4Al_2O_9$ (YAM) traces progressively increased by calcining in the temperature range 850–1350°C;
- Reverse-strike co-precipitation was also a suitable route to produce 50 vol% Al_2O_3–YAG composite powders. In fact, this system yielded pure-YAG phase after calcination at 1215°C for 0 h, while a highly pure-composite product was yielded after calcinations at 1300°C for 0 h;
- In the case of the post-doping procedure, pure alumina–YAG composite powders could be yielded only if suitable thermal and mechanical pre-treatments are set-up. Firstly, a clear lowering of α-Al_2O_3 crystallization temperature was obtained by submitting the just-dried alumina precursor to extensive milling. In addition, it was observed that the lower the pre-treatment temperature of the alumina precipitate, the lower the crystallization temperature of the YAG phase. In fact, the best results were obtained by doping the starting powder and then heat-treating it up to 1200°C to yield the final phases. In addition, yttrium-doping the high-temperature pre-treated alumina (D1-900 and D1-1280) yielded various secondary phases (Y_2O_3, $Y_4Al_2O_9$, $YAlO_3$) which remain up to the higher calcination temperature (namely, up to 1300°C for D1-900 and 1200°C for D1-1280);
- In addition, if D1 and D1-500 powders were submitted to long planetary milling steps, a clear decreasing of hexagonal-$YAlO_3$ and YAG crystallization temperatures was observed after subsequent calcination between 1000 and 1200°C (0-h soaking time). On the contrary, α-Al_2O_3 crystallization was not significantly affected by the extensive milling performed on the doped powders;
- Pure-alumina precursor was partially crystallized as a consequence of the precipitation pH maintained constant at the value set-up for YAG and alumina–YAG materials. However, as a prospective of this work, post-doping could be performed on a completely amorphous precursor, trying to promote a higher homogeneity in the final composite product.

Acknowledgements

The Authors wish to thank the INSTM Consortium to have partially supported this research in the framework of a PRISMA project.

References

1 J. D. French, J. Zhao, M. P. Harmer, H. M. Chan and G. A. Miller, J. Am. Ceram. Soc., 77 (1994) 2857.
2 M. Veith, S. Mathur, A. Kareiva, M. Jilavi, M. Zimmer and V. Huch, J. Mater. Chem., 9 (1999) 3069.
3 S. Ramanathan, M. B. Kakade, P. V. Ravindran, B. B. Kalekar, K. V. Chetty and A. K. Tyagi, J. Therm. Anal. Cal., 84 (2006) 511.
4 S. Ramanathan, M. B. Kakade, S. K. Roy and K. K. Kutty, Ceram. Int., 29 (2003) 477.
5 X. Li, H. Lu, J. Y. Wang, H. M. Cui, F. Han, X. D. Zhang and R. I. Boughton, Mater. Lett., 58 (2004) 2377.
6 Q. Zhang and F. Saito, Powder Technol., 129 (2003) 86.
7 T. Tachiwaki, M. Yoshinaka, K. Hirota, T. Ikegami and O. Yamaguhi, Solid State Commun., 119 (2001) 603.
8 W. Q. Li and L. Gao, Nanostruct. Mater., 11 (1999) 1073.
9 H. Wang and L. Gao, Ceram. Int., 27 (2001) 721.
10 A. Ikesue, I. Furusato and K. Kamata, J. Am. Ceram. Soc., 78 (1995) 225.
11 P. Apte, H. Burke and H. Pickup, J. Mater. Res., 7 (1992) 706.
12 J. G. Li, T. Ikegami, J. H. Lee and T. Mori, J. Am. Ceram. Soc., 83 (2000) 961.
13 G. Xu, X. Zhang, W. He, H. Liu, H. Li and R. I. Boughton, Mater. Lett., 60 (2006) 962.
14 H. Wang, L. Gao and K. Niihara, Mater. Sci. Eng., A288 (2000) 1.
15 M. V. Mathieu, Contribution a l'étude des gels d'alumine désorganisée, Ph.D. Thesis, University of Lyon, 1956.
16 A. C. Pierre and D. R. Uhlman, J. Am. Ceram. Soc., 70 (1987) 28.
17 B. E. Yoldas, J. Am. Ceram. Soc., 65 (1982) 387.
18 P. Palmero, C. Esnouf, L. Montanaro and G. Fantozzi, J. Eur. Ceram. Soc., 25 (2005) 1565.
19 O. Yamaguchi, K. Takeoka, K. Hirota, H. Takano and A. Hayashida, J. Mater. Sci. Lett., 27 (1992) 1261.
20 P. Palmero, A. Simone, C. Esnouf, G. Fantozzi and L. Montanaro, J. Eur. Ceram. Soc., 26 (2006) 941.
21 E. Calvet, P. Boinvinet, M. Noël, H. Thibon, A. Maillard and R. Tertian, Bull. Soc. Chim. Fr., 20 (1953) 99.

DOI: 10.1007/s10973-006-8010-7